The resonant multi-pulse ionization injection

Paolo Tomassini,[1,a)] Sergio De Nicola,[2,3] Luca Labate,[1,4] Pasquale Londrillo,[5] Renato Fedele,[2,6] Davide Terzani,[2,6] and Leonida A. Gizzi[1,4]
[1]*Intense Laser Irradiation Laboratory, INO-CNR, 56124 Pisa, Italy*
[2]*Dip. Fisica Universita' di Napoli Federico II, 80126 Napoli, Italy*
[3]*CNR-SPIN, Napoli, 80126 Napoli, Italy*
[4]*INFN, Sect. of Pisa, 56100 Pisa, Italy*
[5]*INAF, 40129 Bologna, Italy*
[6]*INFN, Sect. of Napoli, 80126 Napoli, Italy*

(Received 17 August 2017; accepted 14 September 2017; published online 5 October 2017)

The production of high-quality electron bunches in Laser Wake Field Acceleration relies on the possibility to inject ultra-low emittance bunches in the plasma wave. In this paper, we present a new bunch injection scheme in which electrons extracted by ionization are trapped by a large-amplitude plasma wave driven by a train of resonant ultrashort pulses. In the Resonant Multi-Pulse Ionization injection scheme, the main portion of a single ultrashort (e.g., Ti:Sa) laser system pulse is temporally shaped as a sequence of resonant sub-pulses, while a minor portion acts as an ionizing pulse. Simulations show that high-quality electron bunches with normalized emittance as low as 0.08 mm × mrad and 0.65% energy spread can be obtained with a single present-day 100TW-class Ti:Sa laser system. *Published by AIP Publishing*. https://doi.org/10.1063/1.5000696

I. INTRODUCTION

High-quality Laser Wake Field Accelerated (LWFA) electron bunches are nowadays requested for several applications including free electron lasers,[1–3] X/γ sources,[4–8] and staged acceleration.[9–13] While performances of self-injected bunches generated in the so-called bubble regime[14,15] continue to improve, other promising injection schemes, including injection via density downramp,[16–20] colliding pulses injection,[21–23] and ionization injection,[24–32] are under active theoretical and experimental investigation.

Evolution of the ionization injection, based on the use of two laser pulses (either with the same or different wavelengths), was proposed in Refs. 33–36. In the two-color ionization injection,[34] the main pulse that drives the plasma wave has a long wavelength, five or ten micrometers, and a large normalized amplitude $a_0 = eA/mc^2 = 8.5 \times 10^{-10}\sqrt{I\lambda^2} > 1$, being I and λ the pulse intensity in $\mathrm{W/cm^2}$ and the wavelength in μm. The second pulse (the "ionization pulse") possesses a large electric field though its normalized amplitude is low. This is achieved by doubling the fundamental frequency of a Ti:Sa pulse. While the main pulse cannot ionize the electrons in the external shells of the contaminant species due to its long wavelength, the electric field of the ionization pulse is large enough to generate newborn electrons that will be trapped in the bucket. This opens the possibility of using gas species with relatively low ionization potentials, thus enabling separation of wake excitation from particle extraction and trapping.

Two color ionization injection is in fact a flexible and efficient scheme for high-quality electron bunch production. The main drawbacks of the two color ionization injection are the current lack of short (T<100 fs) 100TW-class laser systems operating at large (≈10μm) wavelength and lasers synchronization jitter issues. These limitations make the two-color scheme currently unpractical for application to LWFA-based devices requiring high quality beams.

In this paper, we propose a new injection configuration (Fig. 1) (we will refer to it as Resonant Multi-Pulse Ionization injection, ReMPI) that overcomes these limitations and opens the way to a reliable generation of high quality Laser Wakefield accelerators. The breakthrough of our ReMPI scheme consists in the replacement of the long wavelength high peak power driving pulse of the two-color scheme with a short wavelength, resonant multi-pulse laser driver. In fact, due to the resonant enhancement of the ponderomotive force, a properly tuned train of pulses[37–39] is capable of driving plasma waves with larger amplitude than a single pulse with the same energy. In such a way, given the much lower intensity of the driving pulses, it is possible to match the conditions of *both* particle trapping and unsaturated ionization of the active atoms level. Notably, such a driver can be obtained via temporal shaping techniques from a *single*, linearly polarized, standard CPA laser pulse. A minor fraction of the same pulse can be frequency doubled

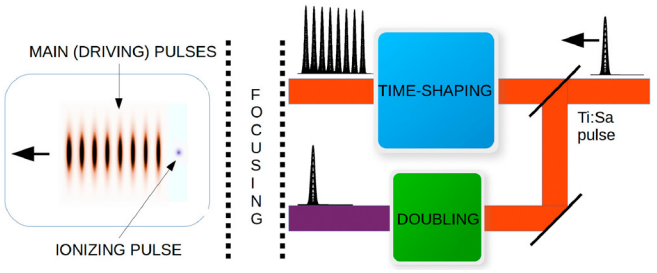

FIG. 1. Resonant Multi-Pulse Ionization injection scheme. A small fraction of a single Ti:Sa laser pulse is frequency doubled and will constitute the ionizing pulse. The main portion of the pulse is temporally shaped as a train of resonant pulses that will drive a large amplitude plasma wave.

a)paolo.tomassini@ino.it

(or tripled) and used as the ionizing pulse. Recently,[40,41] exciting experimental results on the generation of such a time shaped pulses demonstrate that a multi pulse scheme is obtainable with present day technology.

The paper is organized as follows. In Sec. II, we recall the resonant multi-pulse wakefield excitation comparing it with typical single pulse excitation conditions. In Sec. III, we set-up trapping conditions for electrons extracted in a plasma wave driven by a resonant train of pulses designed for a state-of-the-art 250TW Ti:Sa laser system. In Sec. IV, we will discuss in detail the process of electron extraction by a linearly polarized ultraintense pulse. We carried out extensive numerical simulations to evaluate applicability and robustness of the scheme. In Sec. V, we will report on the simplest case of un-guided pulses designed for a state-of-the-art 250TW Ti:Sa laser system. Finally, Sec. VI is devoted to discussion of the results obtained by our simulations. In the Appendices details on the ADK ionization model will be found, along with a description of the hybrid fluid/kinetic QFluid code used for the simulations.

II. THE MULTI-PULSE LWFA

The excitation of plasma waves using multiple laser pulses rather than a single, higher energy one was first studied, from a theoretical viewpoint, by Umstadter *et al.*[37] and Dalla and Lontano.[38] In this Multi Pulse (MP) option, the Langmuir wave is gradually excited by means of a resonant train of pulses. The Self-Modulated LWFA process (see, among others Refs. 42 and 43), is, for instance, based on such a kind of multi pulse excitation, each short pulse resulting from the self-modulation of a single, long laser pulse with length exceeding the plasma wavelength λ_p.

In a linear regime, the resonant enhancement of the ponderomotive force effect takes place when the pulse-to-pulse delay T_{delay} matches the plasma wave period. When the plasma wave amplitude is relatively high, both the optimal pulse-to-pulse delay T_{delay} and pulse duration can change (even significantly)[37,38] from the simpler case of constant delay $T_{delay} = \lambda_p/c$ given by the linear theory. In that case, a parametric scan for T_{delay} is needed to obtain an efficient resonant regime. On the experimental side, the Multi-Pulse acceleration can be achieved either starting from a set of pulses generated by different laser systems (e.g., from fiber lasers[39] to reach kHz repetition rates) or, as considered in the present paper, from a single pulse passing through a time-shaping device.[40,41]

It is worth noting that, for the excitation of the plasma wave, an optimized train of pulses is more efficient than a single laser pulse with the same duration and delivered energy. As an illustrative example, a comparison between the two cases is shown in Fig. 2 where we report the line outs of the on-axis longitudinal electric field in the cases of excitations by either a single driving pulse or an optimized eight-pulses driving train with the same total energy as the single pulse. Simulations reported were performed with the ALaDyn PIC code[44] in 2D slice geometry and with the QFluid code[45] (see also Appendix B) in 2D *cylindrical* geometry. The QFluid code is the cold-fluid/kinetic code that

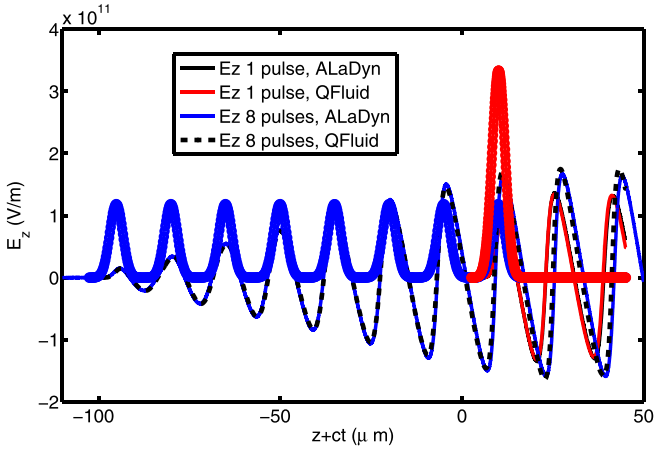

FIG. 2. Single-pulse vs eight-pulses train comparison. Pulses (moving through the left) with a duration of 10*fs* and a waist size of 25 μm are focused in a $n_e = 5 \times 10^{18}$ cm^{-3} plasma. The single-pulse (red thick line) with a peak intensity of 5.9×10^{18}W/cm^2 drives a plasma wave whose maximum accelerating gradient is 20% less than that of the wave excited by the eight-pulses train having the same delivered energy and intensity 7.4×10^{17}W/cm^2. A numerical scan of the pulse-to-pulse-delay has been performed to obtain the resonance condition. QFluid and PIC (ALaDyn 2D) simulation are in excellent agreement.

solves the plasma dynamics in a 2D cylindrical geometry by means of the Quasi Static Approximation.[46] Electron macroparticles move kinetically in a full 3D dynamics depicted by the longitudinal E_z and radial E_r electric field, the azimuthal magnetic field B_ϕ and ponderomotive forces due to laser pulses. The main laser pulse train propagates following the envelope evolution equation with the second time derivative included,[47] while the evolution of the ionization pulse follows the Gaussian pulse evolution prescription. For our purposes, in the absence of non-fluid plasma behavior, strong longitudinal background gradients and radial anisotropies, QFluid returns the same results of a 3D PIC code with much less demanding computation time/resources. In the simulations of Fig. 2, each pulse has a duration of 10*fs* and a waist size of 25 μm and is focused in a plasma having density of $n_e = 5 \times 10^{18}$ cm^{-3}. According to these plots, the eight-pulses train is capable of exciting a plasma wave whose electric field gradient is approximately 20% larger than the peak accelerating gradient of the single pulse.

III. TRAPPING CONDITIONS IN REMPI

To set conditions of particles trapping in the plasma wave, we will focus on a configuration where the longitudinal ponderomotive force dominates over the radial wakefield force, with a train of driving pulses having waist $w_{0,d}$ exceeding the plasma wavelength λ_p. In the 1*D* limit, the Hamiltonian of a passive particle in the plasma wave is[48] $H = (1 + u_z^2)^{1/2} - \beta_{ph} u_z - \phi$, where β_{ph} is the wave phase velocity (transverse contribution to the Lorentz factor has been neglected since relatively low values of the pulse amplitudes will be considered here). The separatrix Hamiltonian H_s decomposes the phase space in a sequence of periodic buckets, so trapping of newborn electrons occurs if the particle Hamiltonian satisfies $H \leq H_s$, i.e., if

$$\phi_e \geq 1 - 1/\gamma_{ph} + \phi_{min} \tag{1}$$

ϕ_e being the normalized electrostatic potential at particle extraction and ϕ_{min} the minimum potential. Equation (1) clearly states that the trapping condition relies on wave phase velocity and on wake electrostatic potential, i.e., on plasma density and normalized electric field $E_{norm} = E_z/E_0$ solely, where $E_0 = mc\omega_p/e$. The exact solution of the fully nonlinear wave equation in the 1D limit gives us a relationship between the normalized electric field and maximum/minimum potential[48] $\phi_{max,min} = E_{norm}^2/2 \pm \beta_{ph}\sqrt{(1+E_{norm}^2/2)^2 - 1}$.

Trapping starts when Eq. (1) holds, i.e., when electrons reach the end of the bucket with the same speed as the wake phase speed ($v = \beta_{ph}c$). Since these electrons will not be accelerated further, we will refer to this condition as a "weak trapping condition"

$$2\beta_{ph}\sqrt{(1+E_{norm}^2/2)^2 - 1} \geq 1 - 1/\gamma_{ph}\,. \tag{2}$$

Moreover, electrons that reach the speed of the wake before they experience the maximum accelerating field will dephase in the early stage of acceleration. As a consequence, a "strong trapping condition" can be introduced in such a way that electrons move with $v = \beta_{ph}c$ when they are in phase with the maximum longitudinal accelerating field. In this case the potential at $E_z = E_{max}$ is null, so we get

$$E_{norm}^2/2 + \beta_{ph}\sqrt{(1+E_{norm}^2/2)^2 - 1} \geq 1 - 1/\gamma_{ph}\,. \tag{3}$$

Trapping analysis (see Fig. 3) reveals that efficient trapping occurs in a nonlinear wave regime since $E_{norm} \approx 0.5$, but far from the deep-nonlinear regime, E_{norm} being well below the longitudinal wavebreaking limit $E_{norm} \ll E_{WB}/E_0 = \sqrt{2(\gamma_{ph}-1)} \gg 1$.[49] Such an analysis is confirmed by our simulations and it is useful to set trapping threshold values for peak pulse normalized amplitude $a_{0,d}$ in single or multi-pulse schemes.

If a plasma density of $n_e = 5 \times 10^{17}\mathrm{cm}^{-3}$ is selected, a matched set of parameters for the driving train gives each pulse duration of $T_d = 30$ fs FWHM, with a minimum waist $w_{0,d} = 45\,\mu$ m (the same parameters set will be used in the 250 TW state-of-the-art simulation, see below). Results of a set of QFluid simulations with a scan of the maximum accelerating field versus pulse normalized amplitude and the number of pulses in the driving train is reported in Fig. 3 (bottom). Three delivered energies of 2.5 J, 5.0 J, and 7.5 J have been considered and, for any of them, a single-pulse, two, four and eight-pulses trains have been simulated. As shown in Fig. 3 (bottom), for a fixed total delivered laser energy, as the number of pulses in the train increases the maximum accelerating gradient of the wave increases due to a resonance enhancement of the wave. Moreover, from Fig. 3 (top and bottom), we can infer that the weak-trapping threshold Eq. (2) is reached with a single-pulse of normalized amplitude exceeding $a_{0,d} = 1.6$, while in the case of an eight-pulses train, weak-trapping threshold normalized amplitude is reduced to $a_{0,d} = 0.5$.

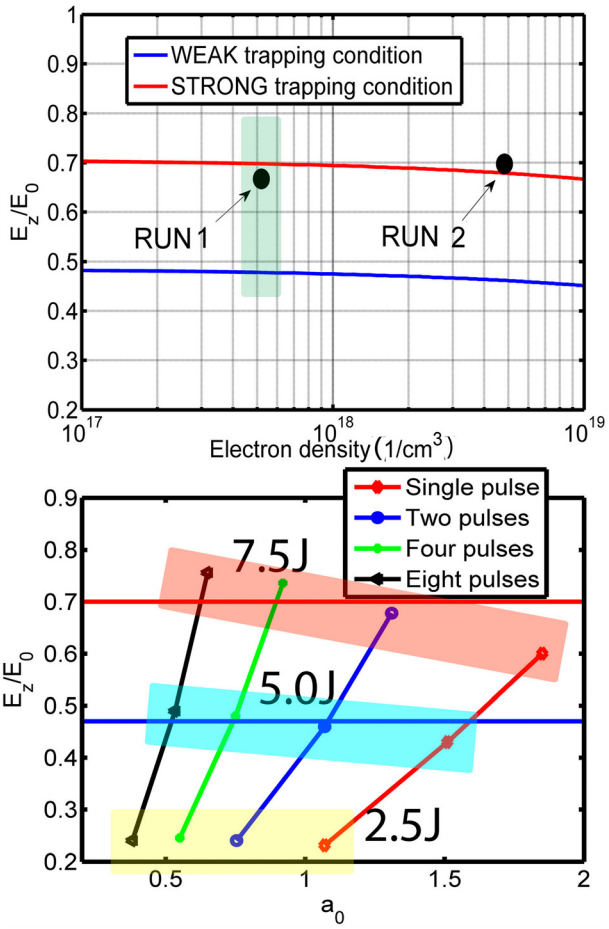

FIG. 3. Trapping conditions. Blue lines: weak trapping threshold; red lines: strong trapping condition. Top: trapping conditions in a 1D nonlinear limit *vs* plasma density from 1D analytical expression Eqs. (2) and (3). RUN 1,2 refer to the working points of the state-of-the-art simulation (Sec. V) and the simulation in Appendix B, respectively. Bottom: scan of maximum accelerating normalized fields as in the RUN 1 setup ($T_d = 30$fs, $n_e = 5\times10^{17}\mathrm{cm}^{-3}$, $w_{0,d} = 45\,\mu$m) as a function of pulse amplitude and the number of pulses in the train. The cases of a single pulse and two, four and eight-pulses trains with three different delivered energies of 2.5J, 5.0J and 7.5J have been considered. A numerical scan with QFluid of the pulse-to-pulse delay has been performed to obtain the resonance condition for each number of pules.

IV. IONIZATION DYNAMICS IN LINEAR POLARIZATION

Ultraintense laser pulses possess electric fields large enough to make tunneling as the dominant ionization mechanism (i.e., Keldysh parameter[50] $\gamma_K = \sqrt{2U_I/mc^2}/a_0 \ll 1$) so the Ammosov-Delone-Krainov (ADK) ionization rate[51] (see also Ref. 52 for a general discussion about the strong laser field ionization) can be assumed to evaluate electron extraction from the initial level (see the Appendix). Ionization potential of 6th electron from nitrogen is $U_I^{6th} = 552$eV and efficient extraction of 6th electron of nitrogen requires $a_0 \approx 1.7$ for a few tens of femtoseconds long pulses at $\lambda = 0.8\,\mu$m. On the other hand, Argon can be ionized from the 8th level to 9th level ($U_I^{9th} = 422.5$eV) at a much lower intensity, where $a_0 \approx 0.8$ and $a_0 \approx 0.4$ with $\lambda = 0.8\mu$m and $\lambda = 0.4\,\mu$m, respectively.

We point out that a detailed description of ionization dynamics is crucial not only to correctly estimate the number

of bunch electrons but (more importantly) to get a precise measure of the transverse phase space covered by newborn electrons. In the linear polarization case, most of the electrons are ejected when the local electric field is maximum, i.e., when the pulse normalized amplitude a_e (the normalized amplitude at the extraction time) is null. These electrons will leave the pulse with a negligible quivering mean momentum along the polarization axis x. If newborn electrons leave the atom when electric field is not exactly at its maximum, a non null transverse momentum $u_x = p_x/mc = -a_e$ is acquired, a_e being the local pulse potential at the extraction time. Moreover, ponderomotive forces introduce an axisymmetric contribution to particle transverse momentum. Following Ref. 53, we can write an expression for the *rms* momentum along the x direction as a function of the pulse amplitude *envelope* at the extraction time a_{0e}

$$\sigma_{u_x} \cong \Delta \cdot a_{0e} = \sqrt{a_{0e}^3/a_c}, \tag{4}$$

where $a_c = 0.107(U_I/U_H)^{3/2}\lambda$ is a critical pulse normalized amplitude and $\Delta = \sqrt{a_{0e}/a_c}$ [see Eqs. (7) and (10) in Ref. 53]. Equation (4) gives us an accurate estimate of the minimum transverse momentum obtainable by the ionization process.

Trapping analysis with a standard *single* driving pulse shows that nitrogen could be used in a simplified ionization injection (as suggested in Ref. 34). Since efficient ionization threshold for N^{6+} is $a_{0,d} \approx 1.7$ for $\lambda_d = 0.8\,\mu$m, a small interval of $1.6 < a_{0,d} < 1.7$ for the pulse normalized amplitude is suitable for both trapping and ionization purposes. Such a simplified scheme could be useful either for demonstration purposes or to obtain a controlled injection for good-quality bunches without ultra-low emittance requirements. A two-pulses driver is a far better choice since an optimal pulse normalized amplitude $1.1 < a_{0,d} < 1.3$ allows us to strongly inhibit driver pulses ionization. Using argon ($Ar^{8+} \rightarrow Ar^{9+}$) as a contaminant instead of nitrogen gives us a drastic reduction of transverse particle momentum since the ionization level is saturated with an ionizing pulse with normalized amplitude above $a_{0,i} = 0.4$ at $\lambda_i = 0.4\,\mu$m. Multi-pulse ionization injection with argon; however, requires trains with at least four pulses since the normalized pulse amplitude should not exceed $a_{0,d} = 0.8$ at $\lambda_d = 0.8\,\mu$m (see Fig. 3).

V. STATE-OF-THE-ART 250 TW SIMULATION

The reported simulation (RUN 1) of our Resonant Multi-Pulse Ionization injection is based upon a linearly polarized Ti:Sa laser pulse that is initially split into the ionizing pulse and the eight-pulses driver train, each sub-pulse being 30 fs FWHM in duration and delivering 895 mJ of energy, with a maximum pulse amplitude $a_{0,d} = 0.64$ and minimum waist size $w_{0,d} = 45\,\mu$ m. In the present working point, consisting of a relatively low number of pulses that drive a weakly nonlinear plasma wave, the optimal pulse-to-pulse delay used for the simulation $T_{delay} = 1.015 \times \lambda_p/c$ differs of a most a few percent from the linear one.

The uniform plasma electron density is set to $n_e = 5 \times 10^{17}$ cm^{-3} (plasma wavelength is $\lambda_p = 46.9\,\mu$m), obtained with a pure argon pre-ionized up to the 8th level. The frequency doubled component (the "ionizing pulse") with wavelength $\lambda_i = 0.4\,\mu$m, amplitude $a_{0,i} = 0.41$ and duration $T_i = 38$ fs is focused with a waist $w_{0,i} = 3.5\,\mu$m. The QFluid simulation (see Fig. 4) has been performed in a moving cylinder having a radius $4 \times w_0$ with a resolution of $\lambda_p/100$ and $\lambda_p/200$ in the radial and longitudinal coordinates, respectively.

Electrons extracted in the bulk of the ionizing pulse move suddenly backwards in the wake reaching the peak of the accelerating gradient of relative intensity $E_{norm} = E_z/E_0 = 0.685$, i.e., very close to the strong-trapping condition (see Fig. 3). Even though the driving pulse sequence generates a marginal further ionization of Ar^{8+} with a maximum percentage ionization of about 3%, such a dark current will not be trapped in the wake (particles are extracted away from the optimal extraction point of maximum potential ϕ_{max}) and so it will have no detrimental effect on beam quality. Moreover, the short Rayleigh length $Z_R = \pi w_{0,i}^2/\lambda_i \approx 100\,\mu$m ensures a sudden truncation of beam charging that turns into a small rms absolute energy spread $\Delta E \approx E_{norm} \times E_0 \times Z_R \approx 5$ MeV and extracted charge $Q = 3.8$ pC.

At the end of beam charging, i.e., after about 200 μm of propagation, the *rms* bunch length is 0.56 μ m and the transverse normalized emittance is $\epsilon_{n,x} = 0.070$ mm × mrad in the polarization direction x and $\epsilon_{n,y} = 0.016$ mm × mrad along the y direction. Afterwards, the *quasi-matched* beam

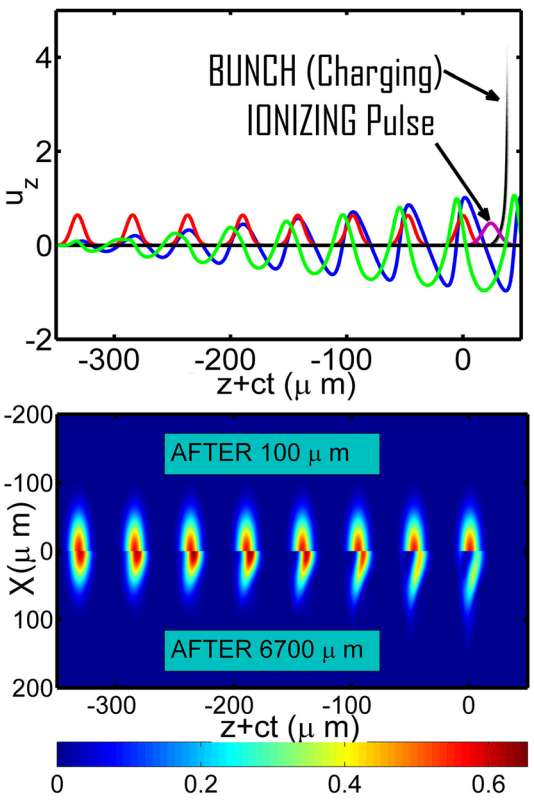

FIG. 4. QFluid Snapshot after 100 μm of propagation and after 6.5 mm. Top: (after 100 μm) lineout of the pulses amplitudes (red/purple lines), accelerating gradient (blue line) fluid longitudinal momentum (green line) and extracted particle's longitudinal phase-space. Electrons ejected by the driving pulse train do not comply with trapping conditions and move as a (quasi) fluid. Bottom: laser pulse amplitude comparison after 100 μm (upper) and after 6.5 mm (lower).

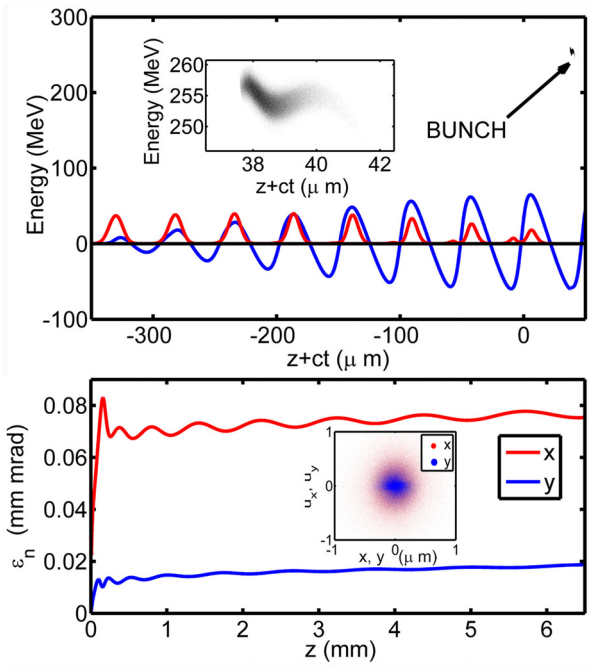

FIG. 5. Bunch quality. Top: Final longitudinal position-energy distribution. Blue and red lines represent the accelerating gradient and pulse amplitude on axis on a.u., respectively. Inset: zoom of the longitudinal phase space. Bottom: Normalized emittance in mm × mrad as bunch moves into the wake. Inset: final transverse phase space.

experiences dumped betatron oscillations with a converging beam radius of 0.4 μm that generates an emittance growth of about 10% as simulation ends (see Fig. 5).

Since in the weak nonlinear regime there is no electron density cavitation as in the bubble regime, beam loading might be a serious limit for beam quality. In the current working point, however, beam loading is present but exerts a tiny perturbation (of about 1%) of the longitudinal field on the bunch core, as it is evident in Fig. 6. We expect, therefore, that the transverse asymmetry of the bunch ($\sigma(x) \approx 2\sigma(y)$) arising from the initial transverse momentum will generate asymmetric beam loading effects but with very low amplitude.

At the end of the 6.5 mm long extraction/acceleration phase, the bunch has mean energy 265 MeV, with final

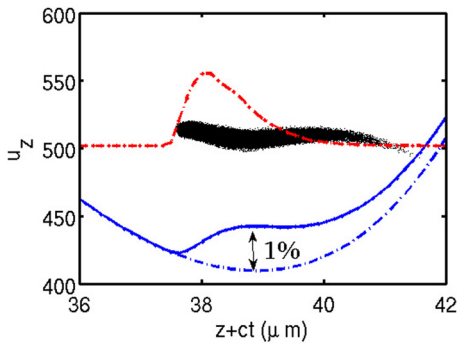

FIG. 6. Beam loading effect at the end of the simulation. The longitudinal phase space of the beam is shown along with the (on axis) beam density (red line), accelerating field (full blue line), and reference field without beam-loading (dashed blue line). Beam loading makes a decrease of the longitudinal field of about 1% at most.

normalized emittances of 0.076 mm × mrad (x axis) and 0.018 mm × mrad (y axis), with an *rms* energy spread 0.65% and the peak current of about 1 kA. These extremely low values of emittance and energy spread show that the proposed Resonant Multi-Pulse Ionization injection scheme is ideal for the generation of very high quality accelerated bunches.

VI. CONCLUSIONS

We described a new, ultra-low emittance, LWFA injector scheme that uses a Resonant train of pulses to drive plasma waves having amplitude large enough to trap and accelerate electrons extracted by ionization. The train of pulses is obtained by temporal shaping of an ultrashort pulse. Unlike the original two-color ionization injection, a *single* laser system (e.g., Ti:Sa) can be therefore employed to both drive the plasma wave and extract newborn electrons by ionization. Simulations consistently show that the main processes, including extraction of electrons due to the ionizing pulse, their trapping in the bucket and subsequent acceleration can be controlled by tuning electron density and laser intensity. Simulations also show a negligible contribution of spurious electrons extracted directly by the driver pulses. Simulations carried out under different plasma conditions show feasibility of the scheme with state-of-the-art-lasers making ReMPI suitable either for direct interaction (e.g., Thomson Scattering or FEL) or as ultra-low emittance injector for GeV-scale energy boosting.

Very recently Cowley *et al.*[41] reported on very encouraging results about the feasibility of their time-shaping setup, with the demonstration of efficient excitation of the plasma wave via Multi-Pulse LWFA. The ReMPI scheme could be tested with two pulses in the train at first, with nitrogen as a contaminant species. In order to obtain very good-quality electron bunches; however, argon should be preferred and in this case more than four pulses in the train are necessary as shown in Sec. III.

ACKNOWLEDGMENTS

The research leading to these results has received funding from the European Union's Horizon 2020 Research and Innovation Program under Grant Agreement No. 653782–EuPRAXIA. The authors also acknowledge financial support from the ELI-ITALY Network funded by CNR. They would like to thank CNAF-INFN for access to computational resources. Finally, the authors acknowledge support from Manuel Kirchen from Hamburg University for his help about the FB-PIC code.

APPENDIX A. ADK IONIZATION RATE

In this paper, we use the following formulation of the instantaneous ADK ionization rate in the tunneling regime:[51]

$$w_{ADK}(|m|) = C \times \rho_{ADK}^{n(|m|)} \times \exp(-1/\rho_{ADK}), \qquad \text{(A1)}$$

where $n(|m|) = -2n^* + |m| + 1$, C is a coefficient depending on the atomic numbers and ionization energy U_I ($U_H = 13.6$eV)

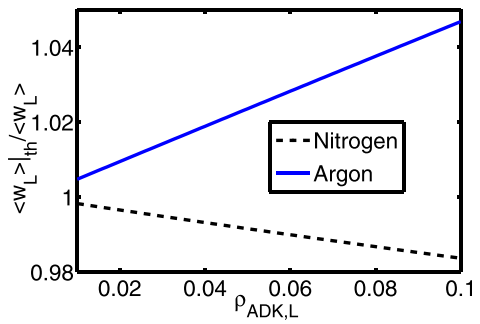

FIG. 7. Comparison between the numerical estimation of the mean-cycled ADK rate and the widely used analytical result of Eq. (A4) for Ar^{9+} and N^{6+} final states.

$$C=\frac{1}{4\pi}\left(\frac{U_I}{U_H}\right)^{3/2}3^{(2n^*-|m|-1)}\left[\frac{4e^2}{n^{*2}-l^{*2}}\right]^{n^*}\left[\frac{n^*-l^*}{n^*+l^*}\right]^{l+\frac{1}{2}}, \quad \text{(A2)}$$

and $\rho_{ADK}=3/2(E/E_{at})(U_H/U_I)^{3/2}$, where $E_{at}=0.514$ TV/m and E the atomic and the local electric fields, respectively. The effective quantum numbers are $n^*=Z\sqrt{U_H/U_I}$ and $l^*=n_0^*-1$, n_0^* being referred to the lower state with the same l. A critical electric field $E_c=2/3E_{at}(U_I/U_H)^{3/2}$, giving a scale of a short-time scale ionization, can be introduced. By expressing E/E_c using vector potentials, we get $a/a_c=\rho_{ADK}=9.37(U_H/U_I)^{3/2}a/\lambda$ which is nothing but the square of Δ parameter in Refs. 53 and 54.

In the circularly polarized pulse case, the electric field rotates within each cycle still retaining the same intensity, so in the tunnelling regime the mean-cycled ionization rate coincides with the instantaneous rate of Eq. (A1)

$$\langle w_c\rangle = w_{ADK}\,. \quad \text{(A3)}$$

In the linearly polarized pulse case, the mean over a cycle can be performed analytically after a Taylor expansion of the leading exponential term. The well-known result (rewritten in our notation) is

$$\langle w_L\rangle = w_{ADK}(\rho_{ADK,0})\times\left(\frac{2}{\pi}\rho_{ADK,0}\right)^{1/2}, \quad \text{(A4)}$$

where $\rho_{ADK,0}$ is the peak value of $\rho_{ADK}=a/a_c$ within the cycle. A numerical estimation of the mean-cycled rate confirms the validity of Eq. (A4) with errors below 4% in the ionization rates, for ρ_{ADK} parameters in the range of interest for ionization injection techniques (see Fig. 7).

APPENDIX B: QFLUID CODE

The 2D *cylindrical*, cold-fluid/kinetic code QFluid solves the plasma dynamic by means of the Quasi Static Approximation.[46] Electron macroparticles move kinetically in a full 3D dynamics depicted by the longitudinal E_z and radial E_r electric field, the azimuthal magnetic field B_ϕ and ponderomotive forces due to laser pulses. The main laser pulse train propagates following the envelope evolution equation with the second time derivative included.[47] Particle extraction from atoms/ions is simulated with an ADK rate including the mean over a pulse cycle, while newborn particles are finally ejected with a random transverse momentum $u_\perp$, whose rms value

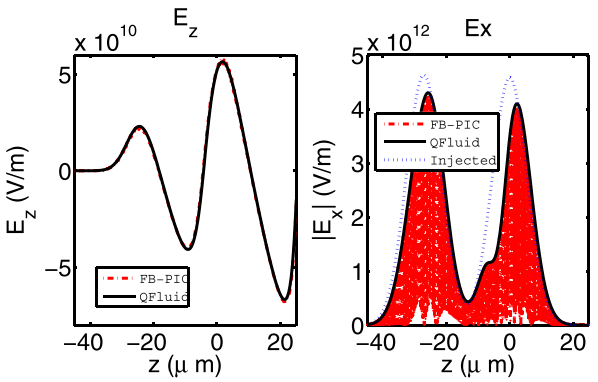

FIG. 8. FB-PIC vs QFluid in a two-pulses driver configuration with nitrogen. Snapshot after 700 μm of propagation into a plasma with background density of $n_e=1.5\times10^{18}\text{cm}^{-3}$. Left: longitudinal electric field on axis. Right: pulse electric field (FB-PIC) and its amplitude (QFluid). The injected pulse amplitude (blue dotted line) has been shown for reference.

depends on the polarization of the pulses. For a linear polarization (as for the ionizing pulse), we assigned $\sigma_{u_x}\cong\Delta\cdot a_{0e}=\sqrt{a_{0e}^3/a_c}$ [see Eq. (4)], while for the circular polarization each extracted particle is associated to a random extraction phase ϕ_e so as $u_x=a_{0e}\times\cos(\phi_e)$, $u_y=a_{0e}\times\sin(\phi_e)$. Benchmark of QFluid with a multi-pulse setup has been obtained in a nonlinear regime with ALaDyn[44] (used here in either a 3D with laser envelope configuration or a 2D slice with a full-PIC pulse evolution) and with FB-PIC (quasi-3D PIC).[55] The comparison of QFluid with FB-PIC is focused on a 2-pulses driver scheme with nitrogen as atomic species. The selected working point consists of linearly polarized pulses of duration $T_d=30$ fs, minimum waist size $w_{0,d}=12\,\mu$m and amplitude $a_{0,d}=1.2$ delayed by a plasma wavelength ($\lambda_p=27\,\mu$m with $n_e=1.5\times10^{18}\text{cm}^{-3}$). FB-PIC simulations were performed with two azimuthal modes, i.e., possible deviation from perfect azimuthal symmetry were included.

The comparison between FB-PIC and QFluid simulation (see Fig. 8) shows a perfect superposition between the codes output, notwithstanding the nontrivial evolution of the pulses due to both nonlinear effects and the variation of the susceptivity due to the wake.

The first QFluid and ALaDyn comparison shown here has been focused on an eight-pulses driver train with argon as atomic species, with selected working point as the same as the state-of-the-art setup. To fasten the 3D PIC simulation, ALaDyn has been equipped with an envelope pulse solver. The ALaDyn/envelope code implements a fully 3D PIC scheme for particle motion whereas the laser pulses are represented by the envelope model proposed in Ref. 56.

Once again (see Fig. 9), QFluid outcomes deviate at most of a few percent from those of a 3D PIC (full 3D in this case).

Finally, a full-PIC (not in envelope approximation) in 2D slice geometry *vs* QFluid comparison, including the bunch extraction and trapping, will be presented (RUN 2). To save computational time, a high-density setup has been simulated. A train of eight 10*fs* linearly polarized Ti:Sa pulses impinge

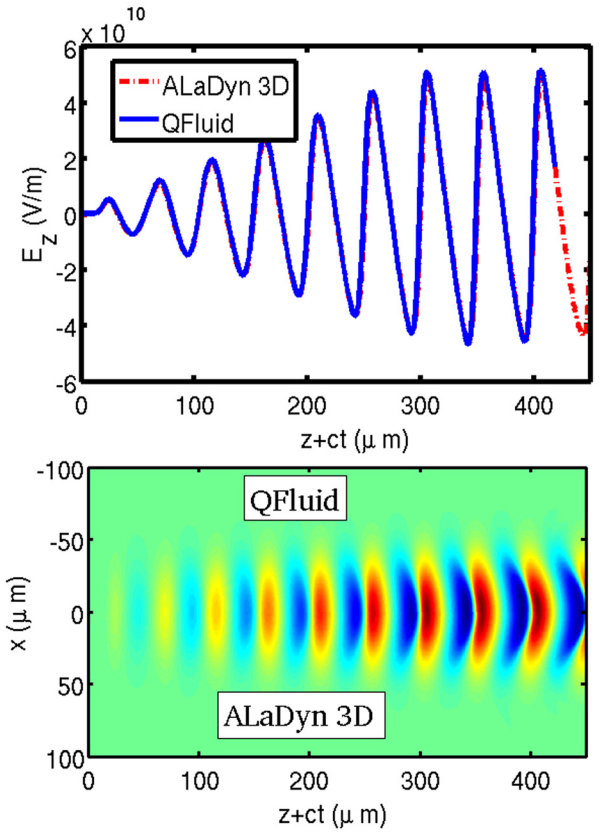

FIG. 9. ALaDyn vs QFluid in an eight-pulses setup with argon (state-of-the-art run parameters). Top: Snapshot of the on-axis longitudinal electric field after 1 mm of propagation. Bottom: radial maps of $E_{norm} = E_z/E_0$ for Qfluid (upper side) vs ALaDyn (lower side).

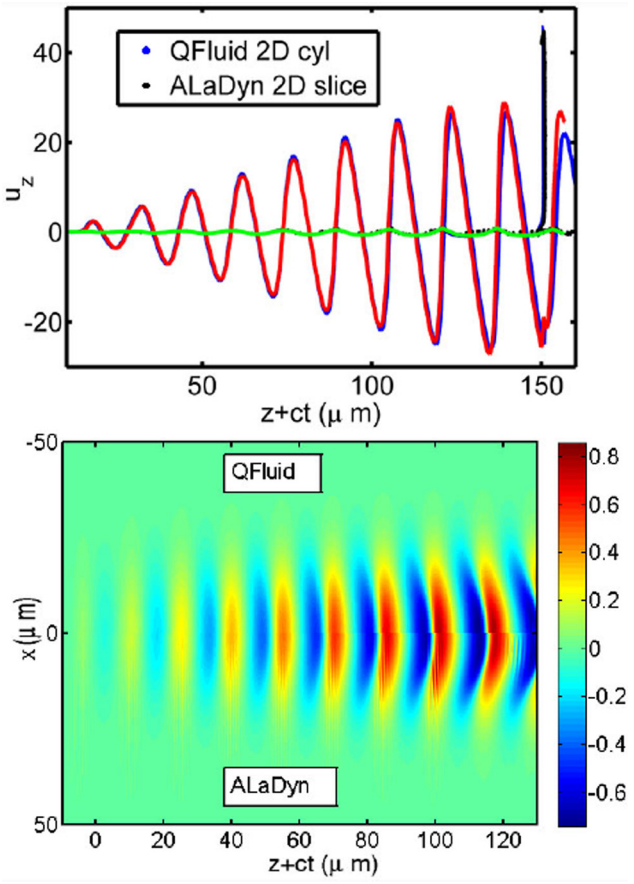

FIG. 10. 2D-slice ALaDyn and QFluid in RUN 2 setup. QFluid and ALaDyn PIC results after 300 μm of propagation. Top: (on-axis) ALaDyn phase space of particles (black dots), QFluid phase space of particles (blue dots), ALaDyn accelerating field (blue line, a.u.), and QFluid accelerating field (red line, a.u.). The green line represents fluid momentum of QFluid output. Bottom: Longitudinal electric field $E_{norm} = E_z/E_0$ from QFluid (upper) and ALaDyn (lower).

onto a preformed plasma of Ar^{8+} with density 5×10^{18} cm^{-3}. The driver pulse train has a waist size $w_{0,d} = 25\,\mu$m and a normalized amplitude $a_{0,d} = 0.589$, having a pulse delay of a single plasma period $T_p = 2\pi/\omega_p$. We use a relatively large focal spot with $w_{0,d} > \lambda_{p,d} = 14.8\,\mu$m, so as to reduce the effects of the missing third dimension in the PIC simulations. The frequency doubled ionizing pulse is injected with a delay of $1.5 \times T_p$ in the vicinity of its focus with a waist $w_{0,i} = 3.5\,\mu$ m and possesses a peak pulse amplitude of $a_{0,i} = 0.41$. PIC simulations were performed with a $170 \times 150\,\mu$m^2 box in the longitudinal and transverse directions with a resolution of $\lambda_d/40$ and $\lambda_d/10$, respectively. QFluid simulations were carried out in the same (cylindrical) box size with resolution $\lambda_p/70$ and $\lambda_p/35$ in the longitudinal and radial coordinates, respectively.

The final snapshot of both simulations, after 300 μm propagation in the plasma is shown in Fig. 10, where the injected electron bunch just at the end of the charging phase is visible (black and blue dots). Due to the large ponderomotive forces (that scale as $a_{0,i}^2/w_{0,i}$, see Eq. (23) in Ref. 53), bunch transverse *rms* momentum (0.26 mc for QFluid and 0.27 mc for ALaDyn, respectively) shows an increase of about a factor of 2 from the value expected by Eq. (4).

We finally stress that QFluid cannot face with the plasma exit of the generated bunch since the Quasi Static Approximation requires a steady plasma density within the box. A PIC code will be used in a future work to simulate the plasma exit, too.

[1]K. Nakajima, "Few femtosecond, few kiloampere electron bunch produced by a laser–plasma accelerator," Nat. Phys. **4**, 92–93 (2008).
[2]V. Petrillo, M. P. Anania, M. Artioli, A. Bacci, M. Bellaveglia, E. Chiadroni, A. Cianchi, F. Ciocci, G. Dattoli, D. D. Giovenale, G. D. Pirro, M. Ferrario, G. Gatti, L. Giannessi, A. Mostacci, P. Musumeci, A. Petralia, R. Pompili, M. Quattromini, J. V. Rau, C. Ronsivalle, A. R. Rossi, E. Sabia, C. Vaccarezza, and F. Villa, "Observation of time-domain modulation of free-electron-laser pulses by multipeaked electron-energy spectrum," Phys. Rev. Lett. **111**, 114802 (2013).
[3]A. Loulergue, M. Labat, C. Evain, C. Benabderrahmane, V. Malka, and M. E. Couprie, "Beam manipulation for compact laser wakefield accelerator based free-electron lasers," New J. Phys. **17**, 023028 (2015).
[4]E. Esarey, S. K. Ride, and P. Sprangle, "Nonlinear Thomson scattering of intense laser pulses from beams and plasmas," Phys. Rev. E **48**, 3003 (1993).
[5]P. Tomassini, A. Giulietti, D. Giulietti, and L. A. Gizzi, "Thomson backscattering x-rays from ultra-relativistic electron bunches and temporally shaped laser pulses," Appl Phys. B **80**, 419–436 (2005).
[6]S. Corde, K. Ta Phuoc, G. Lambert, R. Fitour, V. Malka, A. Rousse, A. Beck, and E. Lefebvre, "Femtosecond x rays from laser-plasma accelerators," Rev. Mod. Phys. **85**, 1 (2013).
[7]V. Petrillo, A. Bacci, C. Curatolo, I. Drebot, A. Giribono, C. Maroli, A. R. Rossi, L. Serafini, P. Tomassini, C. Vaccarezza, and A. Variola, "Polarization of $x-\gamma$ radiation produced by a Thomson and Compton inverse scattering," Phys. Rev. Spec. Top.-Accel. Beams **18**, 110701 (2015).
[8]D. Micieli, I. Drebot, A. Bacci, E. Milotti, V. Petrillo, M. Rossetti Conti, A. R. Rossi, E. Tassi, and L. Serafini, "Compton sources for the observation of elastic photon-photon scattering events," Phys. Rev. Spec. Top.-Accel. Beams **19**, 093401 (2016).

[9]A. Döpp, E. Guillaume, C. Thaurya, A. Lifschitz, K. Ta Phuoc, and V. Malka, "Energy boost in laser wakefield accelerators using sharp density transitions," Phys. Plasmas **23**, 056702 (2016).
[10]S. Steinke, J. Van Tilborg, C. Benedetti, C. G. R. Geddes, J. Daniels, K. K. Swanson, A. J. Gonsalves, K. Nakamura, B. H. Shaw, C. B. Schroeder, E. Esarey, and W. P. Leemans, "Staging of laser-plasma accelerators," Phys. Plasmas **23**, 056705 (2016).
[11]T. L. Audet, F. G. Desforges, A. Maitrallain, S. D. Dufrénoy, M. Bougeard, G. Maynard, P. Lee, M. Hansson, B. Aurand, A. Persson, I. G. González, P. Monot, C.-G. Wahlström, O. Lundh, and B. Cros, "Electron injector for compact staged high energy accelerator," Nucl. Instrum. Methods Phys. Res., Sect. A **829**, 304–308 (2016).
[12]G. Golovin, S. Banerjee, S. Chen, N. Powers, C. Liu, W. Yan, J. Zhang, P. Zhang, B. Zhao, and D. Umstadter, "Control and optimization of a staged laser-wake field accelerator," Nucl. Instrum. Methods Phys. Res., Sect. A **830**, 375–380 (2016).
[13]Z. Zhang, W. Li, J. Liu, W. Wang, C. Yu, Y. Tian, K. Nakajima, A. Deng, R. Qi, C. Wang, Z. Qin, M. Fang, J. Liu, C. Xia, R. Li, and Z. Xu, "Energy spread minimization in a cascaded laser wakefield accelerator via velocity bunching," Phys. Plasmas **23**, 053106 (2016).
[14]J. Faure, Y. Glinec, A. Pukhov, S. Kiselev, S. Gordienko, E. Lefebvre, J.-P. Rousseau, F. Burgy, and V. Malka, "A laser–plasma accelerator producing monoenergetic electron beams," Nature **431**, 541 (2004).
[15]G. R. Plateau, C. G. R. Geddes, D. B. Thorn, M. Chen, C. Benedetti, E. Esarey, A. J. Gonsalves, N. H. Matlis, K. Nakamura, C. B. Schroeder, S. Shiraishi, T. Sokollik, J. van Tilborg, C. Toth, S. Trotsenko, T. S. Kim, M. Battaglia, T. Stöhlker, and W. P. Leemans, "Low-emittance electron bunches from a laser-plasma accelerator measured using single-shot x-ray spectroscopy," Phys. Rev. Lett. **109**, 064802 (2012).
[16]S. Bulanov, N. Naumova, F. Pegoraro, and J. Sakai, "Particle injection into the wave acceleration phase due to nonlinear wake wave breaking," Phys. Rev. E **58**, R5257 (1998).
[17]H. Suk, N. Barov, J. B. Rosenzweig, and E. Esarey, "Plasma electron trapping and acceleration in a plasma wake field using a density transition," Phys. Rev. Lett. **86**, 1011–1014 (2001).
[18]P. Tomassini, M. Galimberti, A. Giulietti, D. Giulietti, L. A. Gizzi, L. Labate, and F. Pegoraro, "Production of high-quality electron beams in numerical experiments of laser wakefield acceleration with longitudinal wave breaking," Phys. Rev. Spec. Top.-Accel. Beams **6**, 121301 (2003).
[19]C. G. R. Geddes, E. Cormier-Michel, E. Esarey, K. Nakamura, G. R. Plateau, C. B. Schroeder, C. Toth, D. L. Bruhwiler, J. R. Cary, and W. P. Leemans, "Plasma gradient controlled injection and postacceleration of high quality electron bunches," in *Proceedings of the Thirteenth Advanced Accelerator Concepts Workshop* (2008), p. 1086.
[20]A. Buck, J. Wenz, J. Xu, K. Khrennikov, K. Schmid, M. Heigoldt, J. M. Mikhailova, M. Geissler, B. Shen, F. Krausz, S. Karsch, and L. Veisz, "Shock-front injector for high-quality laser-plasma acceleration," Phys. Rev. Lett. **110**, 185006 (2013).
[21]E. Esarey, R. F. Hubbard, W. P. Leemans, A. Ting, and P. Sprangle, "Electron injection into plasma wakefields by colliding laser pulses," Phys. Rev. Lett. **79**, 2682 (1997).
[22]H. Kotaki, I. Daito, M. Kando, Y. Hayashi, K. Kawase, T. Kameshima, Y. Fukuda, T. Homma, J. Ma, L. M. Chen *et al.*, "Electron optical injection with head-on and countercrossing colliding laser pulses," Phys. Rev. Lett. **103**, 194803 (2009).
[23]M. Chen, E. Esarey, C. G. R. Geddes, E. Cormier-Michel, C. B. Schroeder, S. S. Bulanov, C. Benedetti, L. L. Yu, S. Rykovanov, D. L. Bruhwiler, and W. P. Leemans, "Electron injection and emittance control by transverse colliding pulses in a laser-plasma accelerator," Phys. Rev. Spec. Top.-Accel. Beams **17**, 051303 (2014).
[24]M. Chen, Z.-M. Sheng, Y.-Y. Ma, and J. Zhang, "Electron injection and trapping in a laser wakefield by field ionization to high-charge states of gases," J. Appl. Phys. **99**, 056109 (2006).
[25]A. Pak, K. A. Marsh, S. F. Martins, W. Lu, W. B. Mori, and C. Joshi, "Injection and trapping of tunnel-ionized electrons into laser-produced wakes," Phys. Rev. Lett. **104**, 025003 (2010).
[26]C. McGuffey, A. G. Thomas, W. Schumaker, T. Matsuoka, V. Chvykov, F. J. Dollar, G. Kalintchenko, V. Yanovsky, A. Maksimchuk, K. Krushelnick *et al.*, "Ionization induced trapping in a laser wakefield accelerator," Phys. Rev. Lett. **104**, 025004 (2010).
[27]C. Thaury, E. Guillaume, A. Lifschitz, K. Ta Phuoc, M. Hansson, G. Grittani, J. Gautier, J.-P. Goddet, A. Tafzi, O. Lundh, and V. Malka, "Shock assisted ionization injection in laser-plasma accelerators," Sci. Rep. **5**, 16310 (2015).
[28]C. E. Clayton, J. E. Ralph, F. Albert, R. A. Fonseca, S. H. Glenzer, C. Joshi, W. Lu, K. A. Marsh, S. F. Martins, W. B. Mori, A. Pak, F. S. Tsung, B. B. Pollock, J. S. Ross, L. O. Silva, and D. H. Froula, "Self-guided laser wakefield acceleration beyond 1 gev using ionization-induced injection," Phys. Rev. Lett. **105**, 105003 (2010).
[29]M. Chen, E. Esarey, C. B. Schroeder, C. G. R. Geddes, and W. P. Leemans, "Theory of ionization-induced trapping in laser-plasma accelerators," Phys. Plasmas **19**, 033101 (2012).
[30]M. Zeng, M. Chen, L. L. Yu, W. B. Mori, Z. M. Sheng, B. Hidding, D. A. Jaroszynski, and J. Zhang, "Multichromatic narrow-energy-spread electron bunches from laser-wakefield acceleration with dual-color lasers," Phys. Rev. Lett. **114**, 084801 (2015).
[31]M. Zeng, J. Luo, M. Chen, W. B. Mori, Z.-M. Sheng, and B. Hidding, "High quality electron beam acceleration by ionization injection in laser wakefields with mid-infrared dual-color lasers," Phys. Plasmas **23**, 063113 (2016).
[32]T. L. Audet, M. Hansson, P. Lee, F. G. Desforges, G. Maynard, S. Dobosz Dufrénoy, R. Lehe, J.-L. Vay, B. Aurand, A. Persson, I. Gallardo González, A. Maitrallain, P. Monot, C.-G. Wahlström, O. Lundh, and B. Cros, "Investigation of ionization-induced electron injection in a wakefield driven by laser inside a gas cell," Phys. Plasmas **23**, 023110 (2016).
[33]N. Bourgeois, J. Cowley, and S. M. Hooker, "Two-pulse ionization injection into quasilinear laser wakefields," Phys. Rev. Lett. **111**, 155004 (2013).
[34]L.-L. Yu, E. Esarey, C. B. Schroeder, J.-L. Vay, C. Benedetti, C. G. R. Geddes, M. Chen, and W. P. Leemans, "Two-color laser-ionization injection," Phys. Rev. Lett. **112**, 125001 (2014).
[35]L.-L. Yu, E. Esarey, C. B. Schroeder, J.-L. Vay, C. Benedetti, C. G. R. Geddes, M. Chen, and W. P. Leemans, "Ultra-low emittance electron beams from two-color laser-ionization injection," AIP Conf. Proc. **1777**, 040019 (2016).
[36]X. L. Xu, Y. P. Wu, C. J. Zhang, F. Li, Y. Wan, J. F. Hua, C.-H. Pai, W. Lu, P. Yu, and W. B. Mori, "Low emittance electron beam generation from a laser wakefield accelerator using two laser pulses with different wavelengths," Phys. Rev. Spec. Top.-Accel. Beams **17**, 061301 (2014).
[37]D. Umstadter, E. Esarey, and J. Kim, "Nonlinear plasma waves driven by optimized laser pulse trains," Phys. Rev. Lett. **72**, 1224 (1994).
[38]S. Dalla and M. Lontano, "Large amplitude plasma wave excitation by means of sequences of short laser pulses," Phys. Rev. E **49**, R1819 (1994).
[39]S. M. Hooker, R. Bartolini, S. P. D. Mangles, A. Tunnermann, L. Corner, J. Limpert, A. Seryi, and R. Walczak, "Multi-pulse laser wakefield acceleration: A new route to efficient, high-repetition-rate plasma accelerators and high flux radiation sources," J. Phys. B **47**, 234003 (2014).
[40]R. J. Shalloo, L. Corner, C. Arran, J. Cowley, G. Cheung, C. Thornton, R. Walczak, and S. M. Hooker, "Generation of laser pulse trains for tests of multi-pulse laser wakefield acceleration," Nucl. Instrum. Methods Phys. Res., Sect. A **829**, 383–385 (2016).
[41]J. Cowley, C. Thornton, C. Arran, R. J. Shalloo, L. Corner, G. Cheung, C. D. Gregory, S. P. D. Mangles, N. H. Matlis, D. R. Symes, R. Walczak, and S. M. Hooker, "Excitation and control of plasma wakefields by multiple laser pulse," Phys. Rev. Lett. **119**, 044802 (2017).
[42]K. Nakajima, D. Fisher, T. Kawakubo, H. Naknishi, A. Ogata, Y. Kato, Y. Kitagawa, R. Kodama, K. Mima, H. Shiraga *et al.*, "Observation of ultra-high gradient electron acceleration by a self-modulated intens short laser pulse," Phys. Rev. Lett. **74**, 4428–4431 (1995).
[43]A. Modena, Z. Najmudin, A. E. Dangor, C. E. Clayton, K. A. Marsch, C. Joshi, V. Malka, C. B. Darrow, and C. Danson, "Observation of raman forward scattering and electron acceleration in the relativistic regime," IEEE Trans. Plasma Sci. **24**, 289 (1996).
[44]C. Benedetti, A. Sgattoni, G. Turchetti, and P. Londrillo, "ALaDyn: A high-accuracy pic code for the Maxwell Vlasov equations," IEEE Trans. Plasma Sci. **36**, 1790 (2008).
[45]P. Tomassini and A. R. Rossi, "Matching strategies for a plasma booster," Plasma Phys. Controlled Fusion **58**, 034001 (2016).
[46]P. Sprangle, E. Esarey, and A. Ting, "Nonlinear theory of intense laser-plasma interaction," Phys. Rev. Lett. **64**, 2011–2014 (1990).
[47]P. Sprangle, E. Esarey, and J. Krall, "Self-guiding and stability of intense optical beams in gases undergoing ionization," Phys. Rev. E **54**, 4211 (1996).
[48]E. Esarey and M. Pilloff, "Trapping and acceleration in nonlinear plasma waves," Phys. Plasmas **2**, 1432 (1995).
[49]A. I. Akhiezer and R. V. Polovin, "Theory of wave motion of an electron plasma," Sov. Phys.-JETP **3**, 696–705 (1956).

[50]L. V. Keldysh, "Ionization in the field of a strong electromagnetic wave," Zh. Eksp. Thor. Fiz. **47**, 1945 (1964). [Sov. Phys. JETP **20**, 1307 (1965)].
[51]V. P. Krainov, W. Xiong, and S. L. Chin, "An introductory overview of tunnel ionization of atoms by intense lasers," Laser Phys. **2**, 4 (1992).
[52]V. S. Popov, "Tunnel and multiphoton ionization of atoms and ions in a strong laser field (Keldysh theory)," Phys. Usp. **47**, 855–885 (2004).
[53]C. B. Schroeder, J.-L. Vay, E. Esarey, S. Bulanov, C. Benedetti, L.-L. Yu, M. Chen, C. G. R. Geddes, and W. P. Leemans, "Thermal emittance from ionization-induced trapping in plasma accelerators," Phys. Rev. Spec. Top.-Accel. Beams **17**, 101301 (2014).
[54]J.-W. Geng, L. Qin, M. Li, W.-H. Xiong, Y. Liu, Q. Gong, and L.-Y. Peng, "Nonadiabatic tunneling ionization of atoms in elliptically polarized laser fields," J. Phys. B: At. Mol. Opt. Phys. **47**, 204027 (2014).
[55]R. Lehe, M. Kirchen, I. A. Andriyash, B. B. Godfrey, and J.-L. Vay, "A spectral quasi-cylindrical and dispersion-free Particle-In-Cell algorithm," Comput. Phys. Commun. **203**, 66–82 (2016).
[56]P. Mora and T. M. Antonsen, Jr., "Kinetic modeling of intense, short laser pulses propagating in tenuous plasmas," Phys. Plasmas **4**, 217 (1997).